Hydrogenation of glycolaldehyde to ethylene glycol at 10 K

Killian Leroux, Jean-Claude Guillemin, Lahouari Krim

Hydrogenation of glycolaldehyde to ethylene glycol at 10 K

Killian Leroux[1], Jean-Claude Guillemin[2] and Lahouari Krim[1*]

[1]*Sorbonne Université, CNRS, De la Molécule aux Nano-Objets: Réactivité, Interactions, Spectroscopies, MONARIS, 75005, Paris, France.*
[2] *Univ Rennes, Ecole Nationale Supérieure de Chimie de Rennes, CNRS, ISCR – UMR6226, F-35000 Rennes, France.*

** Corresponding author: Lahouari.krim@Sorbonne-universite.fr*

Abstract

Glycolaldehyde, the simplest sugar, is a complex organic molecule detected in many regions of the interstellar medium (ISM). Although its synthetic routes are fairly well known and consistent with many laboratory studies, queries still arise about its reactivity and its role in the complex chemistry of the ISM. This study shows the surface and bulk hydrogenation of glycolaldehyde at 10 K in order to confirm or invalidate the astrophysical models which suggest that $CHOCH_2OH$ would be a precursor of ethylene glycol through hydrogenation processes occurring on the surface of interstellar dust grains. By coupling IR spectroscopy and mass spectrometry, we show that the formation of $HOCH_2CH_2OH$ from $CHOCH_2OH$ + H solid state reaction occurs, supporting the existence of a chemical link between these two organics in the ISM. This work suggests that while CHO + CH_2OH and CH_2OH + CH_2OH radical recombination would lead to $CHOCH_2OH$ and $HOCH_2CH_2OH$, respectively, the presence of H-atoms in the ISM would be a secondary source to favour ethylene glycol over glycolaldehyde. These results are in good agreement with different astronomical observations which show simultaneous detections of glycolaldehyde and ethylene glycol with an abundance ratio $HOCH_2CH_2OH/CHOCH_2OH$ ranged between 1 and 15.

Key words: astrochemistry – molecular processes – methods: laboratory: solid state – techniques: spectroscopic – ISM: molecules.

1. Introduction

Glycolaldehyde ($CHOCH_2OH$), the simplest and first sugar detected in the interstellar medium is known to be a precursor of biomolecules. Prebiotic organic species such as glyceraldehyde, an aldotriose, and ribose, the sugar component of nucleic acids, could be formed from glycolaldehyde via the formose reaction (Breslow 1959) or other reactions (Islam et al., 2017). Glycolaldehyde has been detected for the first time in 2000 toward the Sagittarius B2(N) cloud (Hollis et al. 2000). Ever since, more than a few astronomical observations reported its detection near the centre of our Galaxy (Hollis et al. 2001; Hollis et al 2004; Halfen et al. 2006; Raquena-Torres et al. 2008) and also outside the galactic centre around G31.41+0.31, a hot molecular core (Beltrán et al. 2009), IRAS 16293-2422, a Class 0 protostellar binary (Jørgensen et al. 2012), NGC 7129 FIRS 2, an intermediate-mass protostar (Fuente et al. 2014) and NGC 1333 IRAS2A, a solar-type protostar (Coutens et al. 2015; Taquet et al. 2015). Glycolaldehyde has also been detected in celestial bodies such as Hale-Bopp (Crovisier et al. 2004), Lovejoy (Biver et al. 2015) and 67P/Churyumov-Gerasimenko (Goesmann et al. 2015) comets.

In parallel to its astronomical detection many groups have investigated the formation and evolution of glycolaldehyde in the ISM. Although, glycolaldehyde may be formed on the Primitive Earth by the formose reaction (Butlerow 1861; Breslow 1959) with the oligomerization of formaldehyde $H_2CO + H_2CO \rightarrow CHOCH_2OH$, in aqueous solution and in the presence of a basic catalyst, such a reaction pathway has to be excluded as it is unlikely in the ISM. Under the extreme conditions of the interstellar environments, laboratory studies have been focused in the formation and destruction of glycolaldehyde in ice mixtures in order to mimic the surface reactions occurring in the interstellar dust grains.

Analysis of laboratory studies of the formation of organic molecules in astrophysical contexts shows that glycolaldehyde would be principally formed via the $HCO + CH_2OH \rightarrow CHOCH_2OH$ radical recombination. Such radical precursors are generated by UV or electron irradiation (Gerakines et al. 1996; Bennett and Kaiser 2007; Boamah et al. 2014; Butscher et al. 2015; Boyer et al. 2016; Butscher et al. 2017) of CH_3OH or H_2CO containing ices. In a previous study (Leroux and Krim 2020), we showed, while at 10 K the UV-irradiation of pure methanol ice leads mainly to simple species such as CO, CH_4, HCO and CH_2OH, the heating to 100 K favours the consumption of HCO and CH_2OH radicals to form $CHOCH_2OH$. We also showed that the adding of O_2 in the photolysis process of CH_3OH ices leads to $CHOCH_2OH$ oxidization to form CHOCHO. Additionally, glycolaldehyde can also be formed in ice mixtures containing other precursors than CH_3OH and H_2CO. The heating beyond 100 K of the UV-irradiated CH_4–H_2O

ices formed at 10 K reveals the formation of large carbon chain complex organic molecules such as ethanol, propanol and glycolaldehyde (Krim and Jonusas 2019). In addition to the barrierless HCO + CH_2OH radical recombination, theoretical studies (Wood et al. 2013; Fedoseev et al. 2015) suggest that glycolaldehyde can also be formed via the successive hydrogenation of glyoxal (reaction 1a).

$CHOCHO + 2\ H \rightarrow CHOCH_2OH$ (1a)

However, we have experimentally studied the hydrogenation reaction of glyoxal (1a) under interstellar medium conditions. We have shown that glyoxal interaction with H-atoms does not lead to the formation of large complex organic molecules such as glycolaldehyde but it causes the production of smaller species such as CO and H_2CO (Leroux et al. 2020).

Once formed, glycolaldehyde could be a reactive species involved in the chemical complexity of interstellar medium. In this context, laboratory studies have been focused on the destruction of glycolaldehyde under extreme ISM conditions. Hudson et al. (2005) showed that the proton irradiation and warm-up of glycolaldehyde containing ices leads to the formation of small fragments such as CO, CO_2, CH_4, HCO, H_2CO and CH_3OH or of larger species such as ethylene glycol ($HOCH_2CH_2OH$). They have also, but tentatively, detected glyoxal as a photoproduct. In the experimental study carried out by Hudson et al. (2005), we notice that glycolaldehyde exposed to high energy sources leads to photoproducts which may react to form large complex molecules. Although not observed experimentally, H and CH_2OH would be formed during the irradiation of $CHOCH_2OH$ since HCO, H_2CO, CH_3OH are part of the detected photoproducts. Consequently, reaction pathways such as $CH_2OH + CH_2OH$ and $CHOCH_2OH + 2H$ would be the source of $HOCH_2CH_2OH$. In this context, we have investigated the $CHOCH_2OH + 2H$ reaction under ISM conditions in order to confirm or invalidate the formation of ethylene glycol via successive hydrogenation of glycolaldehyde. As we did for the CHOCHO + 2 H reaction which cannot be the main source of $CHOCH_2OH$ in the ISM, we have investigated whether there is a chemical link between $CHOCH_2OH$ and $HOCH_2CH_2OH$ through hydrogenation processes. Although CHOCHO is not yet detected in the ISM, $CHOCH_2OH$ and $HOCH_2CH_2OH$ were observed and generally in the same astronomical regions which suggests a connection between both species. First detected toward Sgr B2 (N-LMH) (Hollis et al. 2002), ethylene glycol has also been detected in the Class 0 protostellar binary IRAS 16293-2422 (Jørgensen et al. 2012). More recently, this diol has been detected toward the solar-type protostar NGC 1333 IRAS2A (Maury et al. 2014), toward the intermediate-mass protostar NGC 7129 FIRS 2 (Fuente et al. 2014) and around the IRc2 region in Orion-KL (Brouillet et al. 2015). As for glycolaldehyde, ethylene glycol has also been detected in comets such as Hale-

Bopp (Crovisier et al. 2004), Lemon, Lovejoy (Biver et al. 2014) and 67P/Churyumov-Gerasimenko (Le Roy et al. 2015).

While CHOCHO + 2 H reaction leads under ISM conditions to CO and H_2CO fragments rather than to $CHOCH_2OH$, is $CHOCH_2OH$ + 2 H reaction also a source of CO and CH_3OH fragments rather than to $HOCH_2CH_2OH$? The aim of the present study is to provide an answer to this issue by performing the hydrogenation of glycolaldehyde at 10 K in order to list the reaction products formed during $CHOCH_2OH$ + 2 H process and their evolution in the 10-300 K temperature range.

2. Experimental section

Glycolaldehyde dimer (99.0 % purity) and ethylene glycol (99.8 % purity) were purchased from Sigma Aldrich and hydrogen (99.9995 % purity) from Messer. The experimental setup used for the present study has been described in our previous article (Leroux et al. 2020). To form glycolaldehyde or ethylene glycol ices at 10K, the organics are first introduced into injection ramps, the pressures of which are controlled by digital Pirani gauges. Due to the low vapor pressures of glycolaldehyde and ethylene glycol at room temperature, the injection ramps were heated to 80 ° C to increase and monitor the amounts of the species to be injected in the reaction chamber. The heating also allowed to vaporize the glycolaldehyde monomer instead of the dimer. Using a Quadrupole Mass Spectrometer (QMS - Hidden Analytical), we have recorded the mass spectra of pure glycolaldehyde and ethylene glycol in order to be certain that the heating of the injection ramps does not lead to a fragmentation of the reactive compounds during the sample deposition. Monitored by leak valves, a closed-cycle helium cryogenerator (Sumitomo cryogenics F-70) and a programmable temperature controller (Lakeshore 336), the reactants prepared in the gas phase are then condensed on a Rh-plated copper mirror maintained at 10 K under ultrahigh vacuum (10^{-10} mbar). H-atoms are produced via a microwave driven atomic source (SPECS, PCS-ECR) by the dissociation of molecular hydrogen H_2. The H_2 dissociation yield of 15 % is measured with a mass spectrometer by monitoring the H and H_2 mass signals with the microwave discharge on and off. The H/H_2 mixture is then injected in the reaction chamber at an optimum pressure of 1.5×10^{-5} mbar with an H-atom flux calculated around 1×10^{17} atoms cm^{-2} s^{-1}. The H-atom flux has not been measured but estimated from the amount of molecular hydrogen injected during the 30 min of the H-bombardment. A curved Teflon tube is added to the microwave discharge in order to block the light from the plasma discharge to avoid possible photo-irradiation processing during the hydrogenation processes and also to thermalize the species released from the atomic source. Although we do not have

access to the amount of H-atoms reaching the substrate where the glycolaldehyde ice is deposited, the surface H + H recombination to form H_2 would decrease considerably the amount of the H-atoms which are involved in the hydrogenation process of the organic molecules. These experimental operating conditions of the atomic source have been optimized from a reference experiment related to the hydrogenation of CO ices to form H_2CO and CH_3OH. The hydrogenation of glycolaldehyde ice has been investigated through two different experiments carried out at 10 K, namely $CHOCH_2OH$ ice bombarded by H atoms and $CHOCH_2OH$ + H simultaneous condensation. While the former illustrates the $CHOCH_2OH$ + H surface reaction where only a few layers of $CHOCH_2OH$ ice are involved in the hydrogenation process which leads to a small amount of reaction products, the latter allows the $CHOCH_2OH$ + H reaction to occur during the sample formation and then to provide an enhancement of the resulting reaction products. The glycolaldehyde ices, before and after hydrogenation are analyzed in the mid-infrared (IR) spectral region between 4000–500 cm^{-1}. Spectra are performed with a resolution of 0.5 cm^{-1}, with an average of 500 scans for each spectrum, using a Bruker Vertex 80v Fourier transform infrared (FTIR) spectrometer in the transmission-reflection mode with an incidence angle of 8° (Pirim & Krim 2011). Additionally, we have recorded IR spectrum of ethylene glycol ($HOCH_2CH_2OH$) ice formed at 10 K under the same experimental conditions. It is taken as a reference spectrum for the potential reaction product we are supposed to obtain during the hydrogenation of $CHOCH_2OH$ ice through $CHOCH_2OH + 2H \rightarrow HOCH_2CH_2OH$ solid state reaction.

After the characterization of the hydrogenation products of glycolaldehyde at 10 K, the solid samples were heated from 10 until 300 K in order to monitor the desorption of glycolaldehyde ice and the resulting $CHOCH_2OH$ + H reaction products via the temperature programmed desorption (TPD) method.

3. Results

Figures 1a and 1b show the infrared spectra of pure glycolaldehyde ice formed at 10 K, before and after hydrogenation, respectively. Table 1 lists the vibrational frequencies and their assignments of glycolaldehyde ice.

Table 1: Assignments of IR absorption bands of pure glycolaldehyde ice

Label[a]	Vibrational mode[a,b]	Present work	Ref[c]
ν18	O-H stretch	3354	3338
ν17	as-CH_2 stretch	2870	2867
ν15	C-H stretch	2819	-
2ν11	Overtone (C-H bend)	2721	2720
2ν8	Overtone (C-O stretch)	2208	-
ν6 + ν8	Combination (C-C stretch + C-O stretch)	1966	-
ν5 + ν8	Combination (O=C-C bend + C-O stretch)	1862	-
ν14	C=O stretch	1745	1747
2ν6	Overtone (C-C stretch)	1706	1706
ν14	CH_2 scissor	1420	1421
ν11	C-H bend	1372	1372
ν10	O-H bend, CH_2 wag	1274	-
ν9	CH_2 twist	1230	1231
ν8	C-O stretch	1107	1108
ν8	C-O stretch	1073	1073
ν8	C-O stretch	1034	-
ν6	C-C stretch	861	861
ν5	O=C-C bend	751	752
ν4	CH_2 rock	713	-

[a] (Carbonniere and Pouchan 2012), [b] (Bleda et al. 2012), [c] (Hudson et al. 2005)

The most characteristic signals of glycolaldehyde ice are the bands at 3354, 1745, and 1107 cm^{-1} corresponding to the O-H, C=O, and C-O stretching modes, respectively. The two spectra of glycolaldehyde ice before and after H-bombardments are quite similar; there is then no evidence for the formation of new reactions products. The absence of CO signal at 2140 cm^{-1} after hydrogenation (Fig. 1b) excludes the $CHOCH_2OH + 2\ H \rightarrow CO + CH_3OH + H_2$ fragmentation, while we showed previously that, under the same experimental conditions, the hydrogenation of CHOCHO ice at 10 K favoured $CHOCHO + 2\ H \rightarrow CO + H_2CO + H_2$ reaction pathways (Leroux et al. 2020).

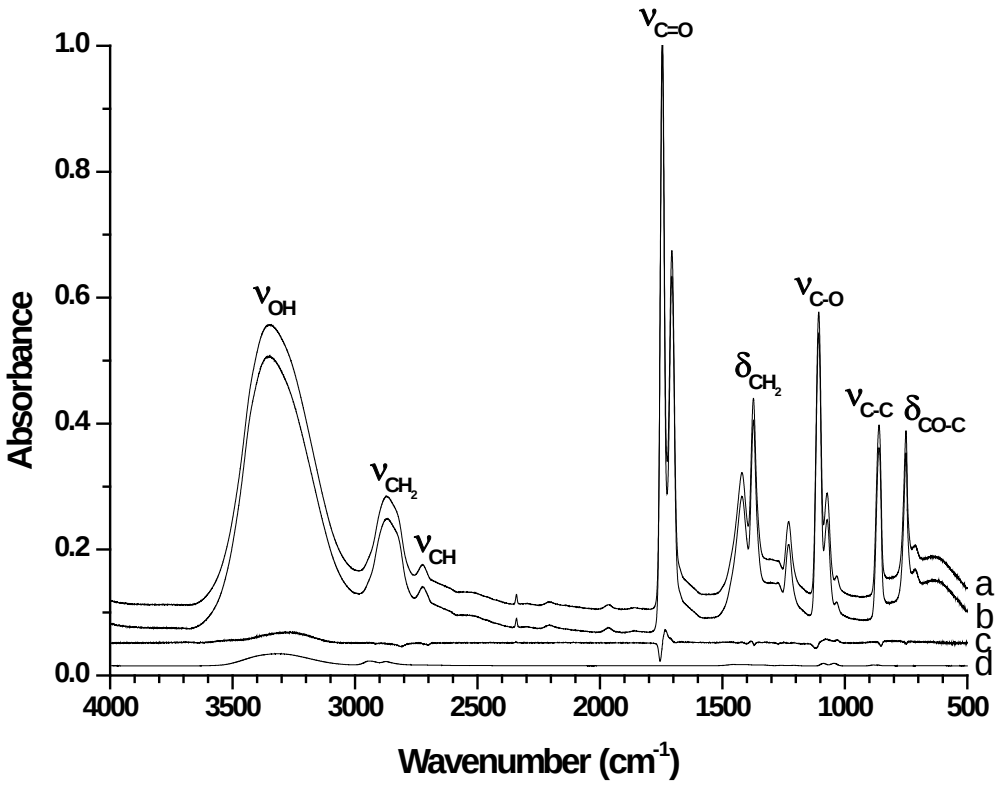

Figure 1: IR spectra of glycolaldehyde ice formed at 10 K (a) before (b) after hydrogenation. (c) Difference spectrum after and before H-bombardments of glycolaldehyde ice (d) reference spectrum of pure ethylene glycol formed at 10 K (the IR signal is divided by 20 in order to be comparable to the difference spectrum).

In order to highlight the $HOCH_2CH_2OH$ formation, the difference spectrum after and before H-bombardments of $CHOCH_2OH$ ice is shown in figure 1c. As a reference spectrum, we have recorded the IR spectrum of ethylene glycol ice formed at 10 K (figure 1d). The IR spectrum of figure 1d is divided by 20 in order to be comparable to the difference spectrum of figure 1c. Figure 2, a zoom of figure 1, focuses on the IR signals of the difference spectrum and those of ethylene glycol ice.

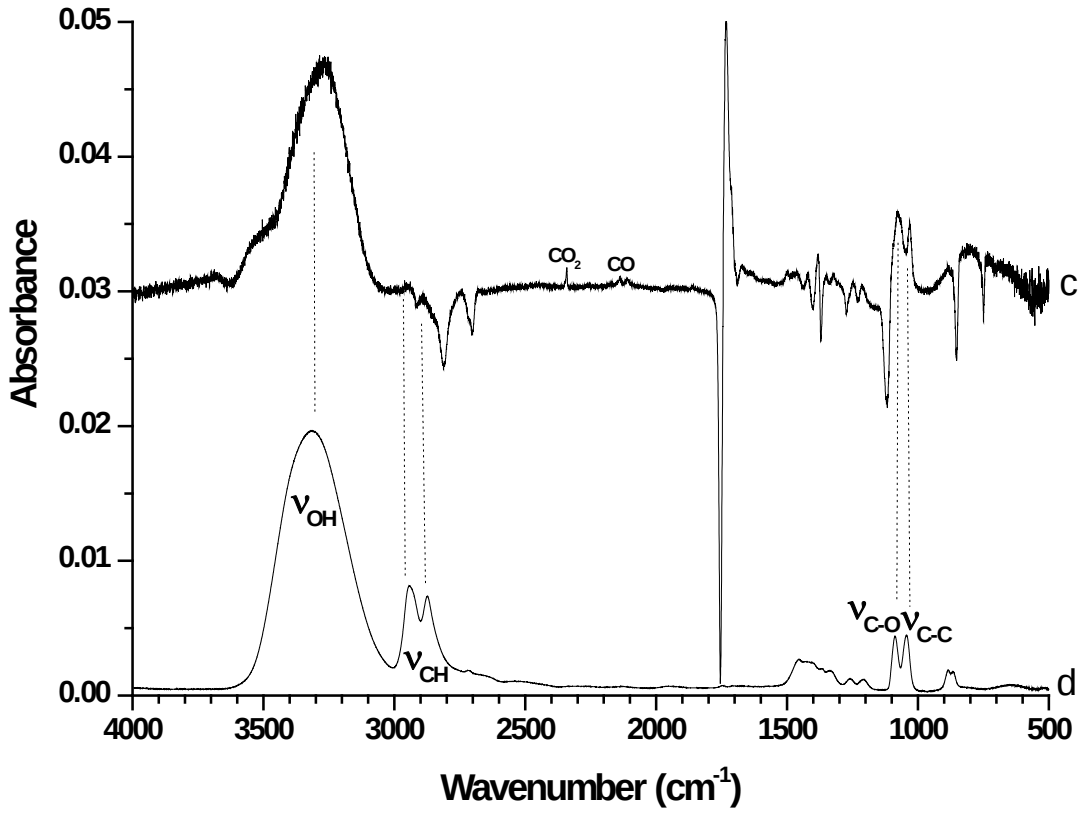

Figure 2: Zoom of figure 1 in 0-0.05 absorption range. (c) Difference spectrum after and before H-bombardments of glycolaldehyde ice (d) reference spectrum of pure ethylene glycol formed at 10 K (the IR signal is divided by 20 in order to be comparable to the difference spectrum).

From figure 2d, we notice that the stronger IR signals and then the most characteristic absorption bands of ethylene glycol ice are located at 3305, 2940, 1090 and 1048 cm^{-1} and they correspond to OH, CH, CO and CC stretching modes (Sawodny et al. 1967; Hudson et al. 2005), respectively. These spectral features of ethylene glycol are also present as positive IR signals in the difference spectrum of figure 2c, proving the formation of $HOCH_2CH_2OH$ through $CHOCH_2OH$ + 2 H reaction, while the negative IR signals in the difference spectrum reveal the amount of glycolaldehyde consumed during the hydrogenation process. However, the potential formation of $HOCH_2CH_2OH$ remains moderate as the H-bombardments are efficient only on the first layers of $CHOCH_2OH$ ice which may limit the yield of the $CHOCH_2OH$ + H reaction. We have then co-injected simultaneously the two reactants H and $CHOCH_2OH$ to form hydrogenated ices with thicknesses similar to those used for the H-bombardment.

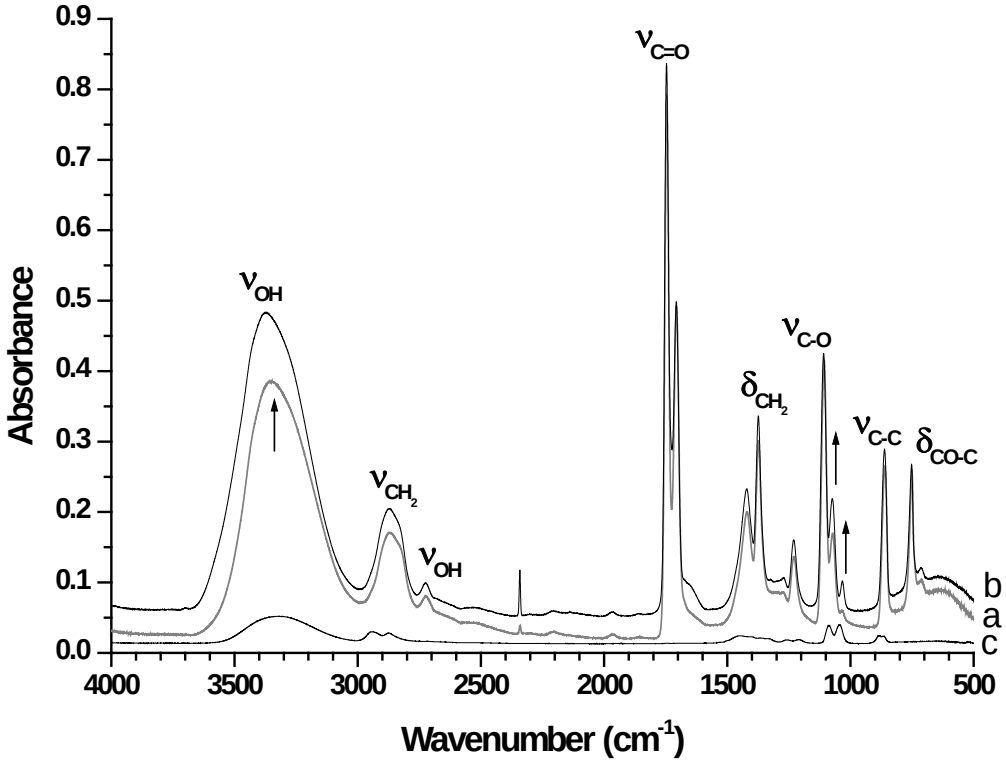

Figure 3: Co-injection experiment at 10 K of a) $CHOCH_2OH + H_2$ and b) $CHOCH_2OH + H/H_2$. c) reference spectrum of pure ethylene glycol formed at 10 K (the IR signal is divided by 20).

Figure 3b shows the IR spectrum resulting from the $CHOCH_2OH + H/H_2$ co-injection at 10 K. As a reference spectrum, figure 3a shows the IR spectrum corresponding to the $CHOCHO + H_2$ co-injection which is similar to the IR spectrum of $CHOCH_2OH$ ice formed at 10 K. The two IR spectra result from two different samples formed at 10 K, consequently, we cannot calculate a difference spectrum to support the formation of ethylene glycol (figure 3c), as we did for the H-bombardments of glycolaldehyde ice (figure 2). However, the comparison between the two spectra (3a and 3b) shows IR signal increases (labelled by arrows in figure 3) around 3360, 1040 and 1080 cm^{-1}, the three spectral regions the most characteristic of $HOCH_2CH_2OH$. However, the overlapping of the IR signals of the products by those of the reactants shows the limits of the IR analysis and we have then used the Thermal Programmed Desorption (TPD) method coupled with mass spectrometry to characterize the reaction products formed in solid phase which evaporate at very specific desorption temperatures. Mass spectra of pure glycolaldehyde, the reactant, and pure ethylene glycol, the potential product, are first recorded in order to select the characteristic mass fragments of each organic species. The characteristic

mass fragments will be monitored in order to investigate the TPD of pure ethylene glycol, pure glycolaldehyde and hydrogenated glycolaldehyde ices.

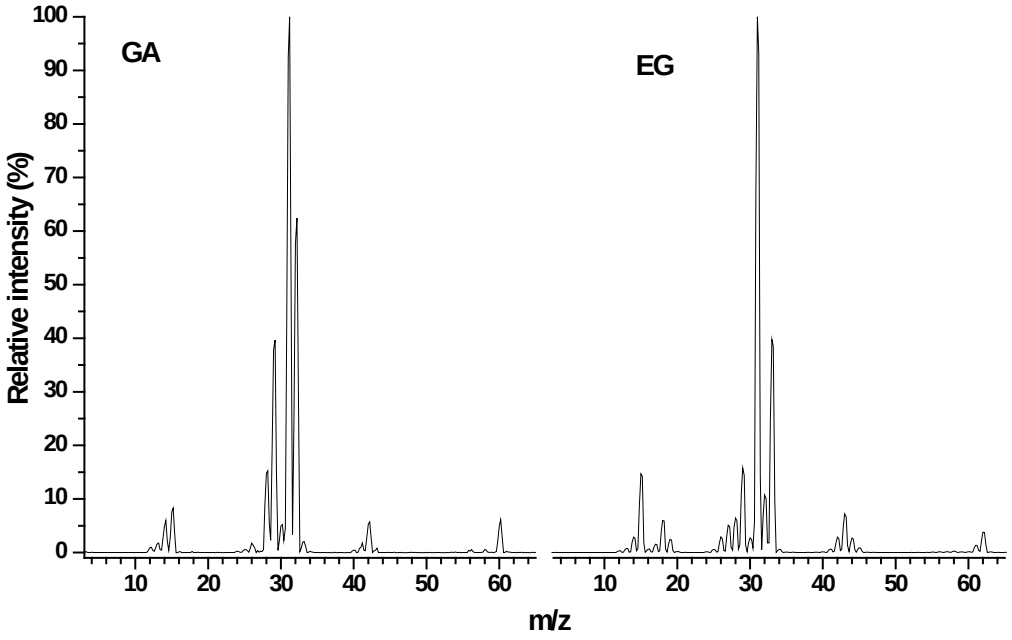

Figure 4: Fragmentation pattern of glycolaldehyde (GA, left) and ethylene glycol (EG, right)

Figure 4 shows the mass spectra of $CHOCH_2OH$ and $HOCH_2CH_2OH$ and Table 2 lists their mass fragments distribution, with the parent species at m/z = 60 and 62, respectively, and most predominate fragment at m/z = 31.

Table 2: Characteristic fragmentation (m/z) of glycolaldehyde and ethylene glycol

Mass	Glycolaldehyde	Ethylene glycol
m/z = 28	15	6
m/z = 29	40	16
m/z = 30	5	3
m/z = 31	100	100
m/z = 32	62	11
m/z = 33	2	40
m/z = 60	6	0
m/z = 62	0	4

In order to characterize the presence of ethylene glycol as one of the products formed through $CHOCH_2OH$ + H reaction, we have chosen to analyse the TPD of ethylene glycol (EG), glycolaldehyde (GA) and hydrogenated glycolaldehyde (GA + H) ices by monitoring fragments at m/z = 33, 60 and 62. Figure 4 shows the TPD spectra of the three ices in the 100-250 K

temperature range. The TPD of glycolaldehyde (GA) ice monitored by the fragment at m/z = 33 shows that pure glycolaldehyde ice starts desorbing at 150 K, reaches a maximum at 189 K and vanishes completely at 200 K. While the TPD of ethylene glycol (EG) ice, monitored by the m/z signal at 62 shows that the desorption process starts at 200 K, it reaches a maximum at 229 K and it ends at 245 K. These results are consistent with glycolaldehyde and ethylene glycol desorption temperatures of 195 and 230 K, respectively, measured in previous studies (Hudson et al. 2005). However, the TPD of the hydrogenated glycolaldehyde (GA + H) ice shows different signals in 150-175, 175-200 and 200-230 K temperature ranges.

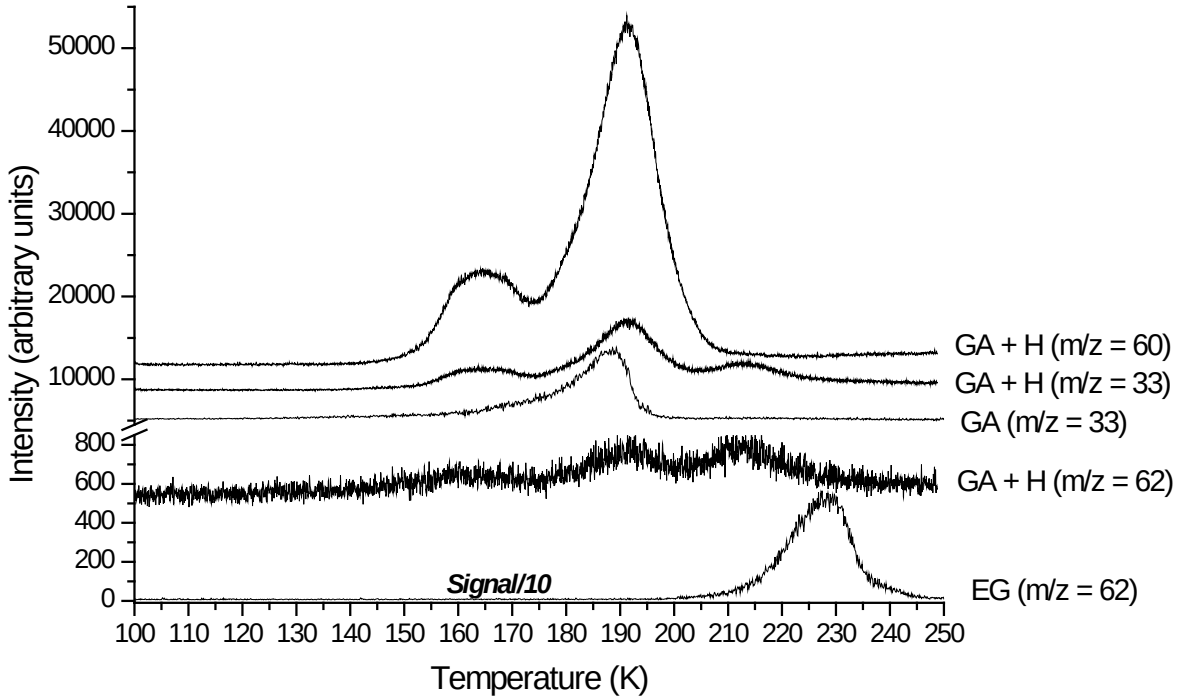

Figure 5: TPD spectra of pure ethylene glycol (EG), pure glycolaldehyde (GA) and hydrogenated glycolaldehyde (GA + H) ices formed at 10 K. The TPD signal of pure EG ice is divided by 10 to be comparable with that of (GA + H) ice.

By analyzing the TPD spectra of the hydrogenated glycolaldehyde (GA + H) ice in the 175-200 K and 200-230 K temperature ranges, the domains of desorption of glycolaldehyde and ethylene glycol, respectively, and the mass signals at m/z = 60, 33 and 62, we show that the hydrogenated glycolaldehyde (GA + H) ice would contain an amount of ethylene glycol which may be formed by $CHOCH_2OH$ + 2 H reaction. However, we notice that in (GA + H) ice, the desorption peak of glycolaldehyde and ethylene glycol molecules are at 192 and 214 K, respectively. Compared to the TPD of pure organic ices, the maximum of the desorption peaks of glycolaldehyde and

ethylene glycol are shifted in the hydrogenated ice (GA + H) by +3 and -15 K, receptively. This temperature shifts are due to the chemical composition of the studied ices. It should be noted that the peak maximum temperature characterizing the desorption of a given chemical species depends strongly on the environment where the species is trapped and also on the amount of species to be desorbed. This would explain the observed differences in the TPD profile of pure EG (m=62) and that of GA+H (m=62). Such differences have already been investigated by many groups (Fuchs et al. 2006, Wolff et al. 2007, Potapov et al. 2018) by studying the evolutions of the shapes and positions of the desorption peaks in the TPD spectra for several pure and mixed ices. During the heating of the hydrogenated sample, small amounts of glycolaldehyde remain maintained by ethylene glycol and this tends to increase the peak maximum temperature of glycolaldehyde by 3 K. Similarly, ethylene glycol formed in small quantity in (GA + H) ice starts desorbing at 200 K and it reaches a maximum at 214 K and disappears completely at 235 K. While in pure ethylene glycol (EG) ice which contains at least 20 times more material (the intensities of the signal at m/z=62 are 210 and 4100 in (GA + H) and EG ices, respectively), the desorption starts at 200 K and ends at 245 K.

As mentioned above, the monitoring of the m/z = 33, 60 and 62 selected fragments for (GA + H) ice shows that the desorption of glycolaldehyde occurs in two steps, in 150 -175 and 175-200 K temperature ranges, while that of ethylene glycol is carried out in three steps with peak maximum temperatures 165, 192 and 214 K. The analysis of the IR spectra of our solid samples shows that at 165 K, the glycolaldehyde ice undergoes an amorphous-to-crystalline phase transition observed through the detection of narrow and sharp absorption bands (figure 6).

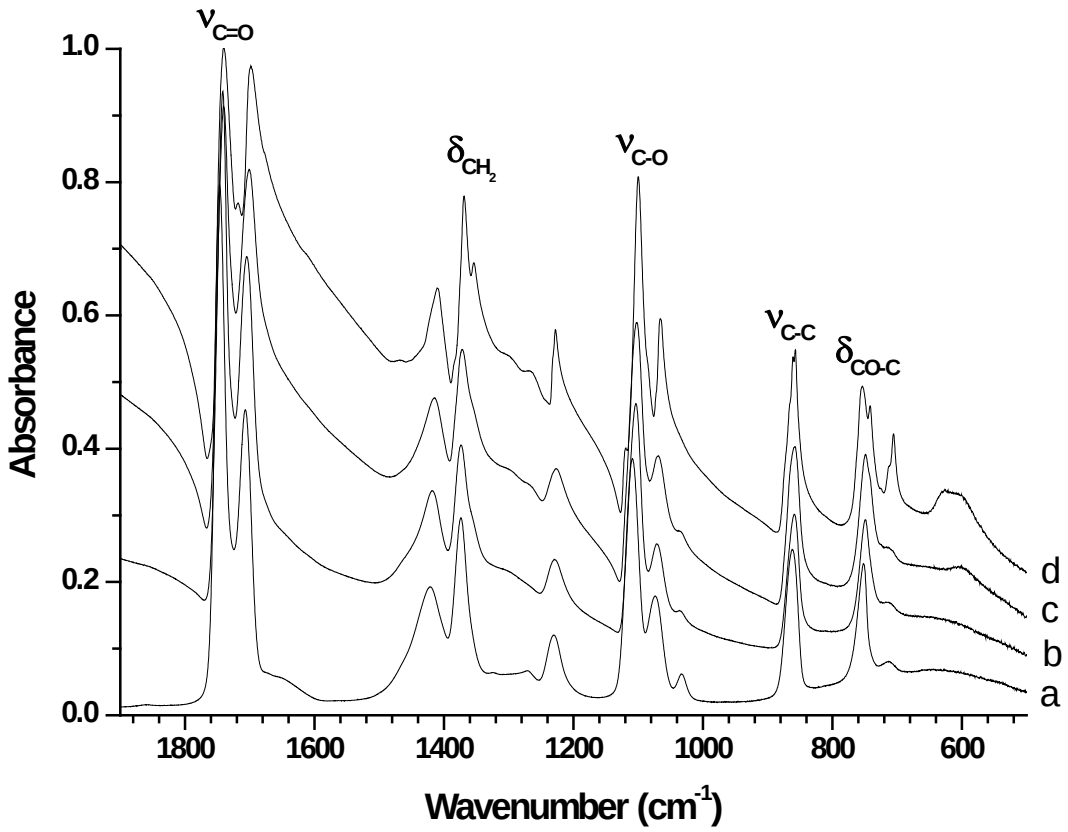

Figure6. IR spectra of hydrogenated glycolaldehyde (GA+H) ice formed at 10K (a) and heated to 155K (b), 160K (c), and165K (d). The ice undergoes an amorphous-to-crystalline phase transition at 165 K.

This phase transition during the sample heating would explain the presence of a shoulder at 165 K in the TPD spectra. Although, less marked, the desorption signal of pure glycolaldehyde ice shows also a shoulder at 168 K related to the amorphous-crystalline phase transition. The observed shoulder becomes more noticeable during the desorption of (GA + H) ice, probably due to the presence of ethylene glycol in the hydrogenated sample. During such a phase transition, species trapped in the ice ($HOCH_2CH_2OH$) and also species forming the ice ($CHOCH_2OH$) may release into the gas phase. Similarly, the reaction product ethylene glycol may also desorb during the hosting ice desorption which occurs in the 175-200 K temperature domain. This may explain why the signals of fragments at m/z = 33, 60 characteristic of glycolaldehyde and those at m/z = 33, 62 characteristic of ethylene glycol are observed in the TPD spectra of the hydrogenated glycolaldehyde ice at 165 and 192 K. At temperatures higher

than 200 K, glycolaldehyde is totally desorbed while ethylene glycol characterized by fragments at m/z= 33, 62, remains in solid phase between 200 and 235 K.

4. Discussion

By coupling infrared analysis and TPD mass spectrometry, we have investigated the $CHOCH_2OH$ + H solid state reaction under simulated ISM conditions. Our results show that that unlike the CHOCHO + H reaction which leads essentially to CO and H_2CO species, the hydrogenation of glycolaldehyde leads mainly to $HOCH_2CH_2OH$ without any fragmentation. This brings a questioning if there is really a link between the unsaturated species CHOCHO and the two organics $CHOCH_2OH$/$HOCH_2CH_2OH$ through reactions involving H-atoms. In a study carried out by Álvarez-Barcia et al. (2018), the $CHOCH_2OH$ + H reaction has been theoretically investigated. They studied the hydrogenation of various functional groups of glycolaldehyde (figure 7), by calculating, for each target site, the barrier heights or activation energies E_a (kJ/mol) in the gas phase which would predict a primary approach to describe the $CHOCH_2OH$ + H surface reaction.

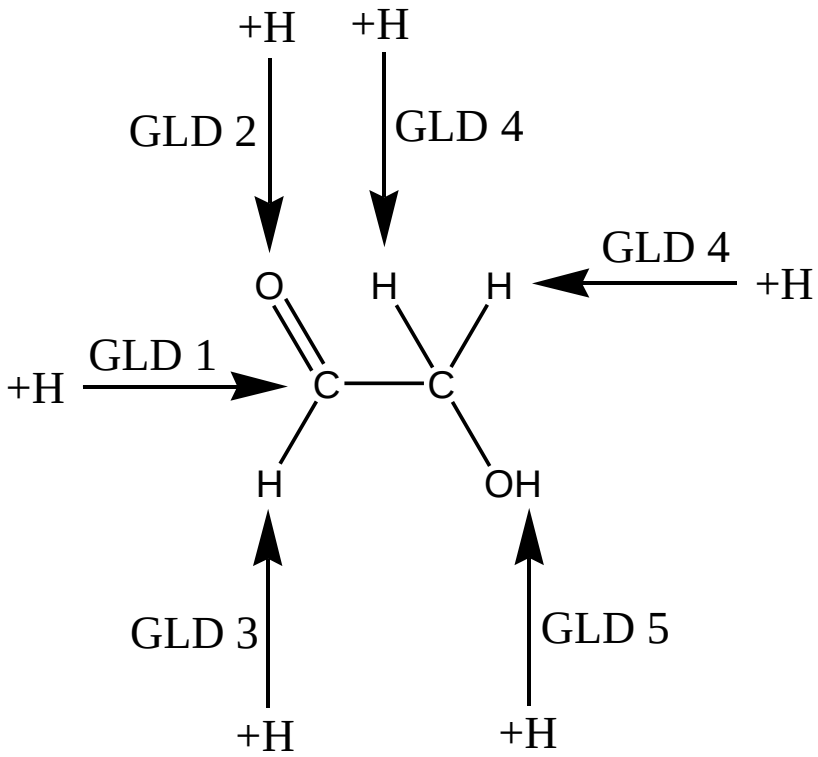

Figure 7: Schematic representation of glycolaldehyde hydrogenation

Álvarez-Barcia et al. (2018) propose that the hydrogenation of glycolaldehyde occurs in five different reaction pathways:

$CHOCH_2OH + H \rightarrow (CH_2O)CH_2OH$	(GLD 1)	E_{a1}= 19.0 kJ mol^{-1}
$CHOCH_2OH + H \rightarrow (CHOH)CH_2OH$	(GLD 2)	E_{a2}= 38.5 kJ mol^{-1}
$CHOCH_2OH + H \rightarrow (CO)CH_2OH + H_2$	(GLD 3)	E_{a3}= 24.3 kJ mol^{-1}
$CHOCH_2OH + H \rightarrow CHOCHOH + H_2$	(GLD 4)	E_{a4}= 27.3 kJ mol^{-1}
$CHOCH_2OH + H \rightarrow CHOCH_2O + H_2$	(GLD 5)	E_{a5}= 55.8 kJ mol^{-1}

The GLD 1 and GLD 2 reactions correspond to the H-addition on the carbon and oxygen of the CHO group, respectively. The two resulting radicals formed are subsequently hydrogenated (reaction GLD 6 and GLD 7) to form ethylene glycol through radical-atom recombination.

$(CH_2O)CH_2OH + H \rightarrow HOCH_2CH_2OH$	(GLD 6)	E_{a6}= 0 kJ mol^{-1}
$(CHOH)CH_2OH + H \rightarrow HOCH_2CH_2OH$	(GLD 7)	E_{a7}= 0 kJ mol^{-1}

However, showing activation energies of 19.0, 38.5 kJ mol^{-1} for GLD 1 and GLD 2 reactions, respectively, the H-addition on the carbon to form $(CH_2O)CH_2OH$ would be a more efficient channel under our experimental conditions.

The GLD 3, GLD 4 and GLD 5 reactions correspond to the H-abstraction from CHO, CH_2 and OH functional groups, respectively. In excess of hydrogen atoms, those radical species react with H-atoms to reform the glycolaldehyde. The activation energies of these reaction pathways are relatively high (24.3, 27.3 and 55.8 kJ mol^{-1}) to be considered in competition with the GLD 1 reaction under non-energetic conditions. Even if they take place, these three processes do not lead to new reaction products but to the reformation of $CHOCH_2OH$ reactant. Consequently, interactions of glycolaldehyde and H-atoms follow a two-step process to produce ethylene glycol via the formation $(CH_2O)CH_2OH$ as reaction intermediate:

$$CHOCH_2OH \xrightarrow{H} (CH_2O)CH_2OH \xrightarrow{H} HOCH_2CH_2OH$$

Once formed, ethylene glycol may interact with H-atoms to favor via H-abstraction processes the reformation of glycolaldehyde and to reach a stationary equilibrium between the formation and the destruction of $HOCH_2CH_2OH$:

$$CHOCH_2OH \underset{-H}{\overset{+H}{\rightleftarrows}} (CH_2O)CH_2OH \underset{-H}{\overset{+H}{\rightleftarrows}} HOCH_2CH_2OH$$

Theoretical studies proposed such reconversion reaction through the hydrogenation of ethylene glycol (Álvarez-Barcia et al. 2018). As ethylene glycol is a saturated species, only hydrogen abstractions from carbon (reaction EG 1) or oxygen (reaction EG 2) sites are possible.

$HOCH_2CH_2OH + H \rightarrow HOCH_2CHOH + H_2$ (EG 1) E_a= 28.4 kJ mol^{-1}

$HOCH_2CH_2OH + H \rightarrow HOCH_2CH_2O + H_2$ (EG 2) E_a= 54.1 kJ mol^{-1}

The high activation energies calculated for these two abstraction reactions show that the hydrogenation of ethylene glycol to retrieve glycolaldehyde would be inefficient under our experimental conditions.

5. Astrophysical implications

As mentioned in the experimental part, the H-atom flux used under our experimental conditions has been estimated around 1×10^{17} atoms cm^{-2} s^{-1} from the amount of molecular hydrogen injected in the microwave discharge. Such a calculated flux leads to H-atom fluences estimated around 2×10^{20} atoms cm^{-2} during the 30 min of the H-bombardment, which is much larger than that expected on dusts in molecular clouds. Although we do not have access to the real amount of H-atoms reaching the substrate where the glycolaldehyde ice is deposited, the H + H surface recombination to form H_2 would decrease considerably the amount of the H-atom fluence on the sample. However, these experimental conditions have been optimized from the reference experiment CO + H solid state reaction to form H_2CO and CH_3OH. We think that the H-atom flux is overestimated in our experiments because by reducing the flux of molecular hydrogen injected in the microwave discharge, we are not able to detect H_2CO or CH_3OH during the hydrogenation of CO-solid and then CO + H reaction becomes inefficient. Although the knowledge of the H-atom fluence remains very important for the astrophysical implication, we investigate here the formation of $HOCH_2CH_2OH$ through $CHOCH_2OH$ + H solid state reaction under the same experimental conditions as for our previous studies devoted to CO + H reaction to characterize the formation of CHO, H_2CO, and CH_3OH (Pirim & Krim, 2011). In such a context, two mechanisms have been proposed to explain the formation of glycolaldehyde and ethylene glycol in solid phase at cryogenic temperatures:

- the radical recombination of CHO• with •CH_2OH to form GA, and the radical •CH_2OH dimerization to form EG.(Butcher et al. 2017).

Mechanism 1:

$$CO \xrightarrow{+H} CHO$$

$$CO \xrightarrow{+H} CHO \xrightarrow{+H} H_2CO \xrightarrow{+H} CH_2OH$$

$$CHO + CH_2OH \rightarrow CHOCH_2OH$$

$$CH_2OH + CH_2OH \rightarrow HOCH_2CH_2OH$$

- the dimerization of formyl radical CHO˙ leading to the formation of glyoxal followed by hydrogenation to form glycolaldehyde and ethylene glycol (Woods et al. 2013; Fedoseev et al. 2015).

Mechanism 2:

$$CHO + CHO \rightarrow CHOCHO$$

$$CHOCHO \xrightarrow{+H} CHOCH_2(O) \xrightarrow{+H} CHOCH_2OH$$

$$CHOCH_2OH \xrightarrow{+H} CH_2(O)CH_2OH \xrightarrow{+H} HOCH_2CH_2OH$$

The mechanism 1 presents the advantage of answering several questions. •CH_2OH is thermodynamically more stable (by ~ 40 kJ/mol) than the CH_3O• isomer (Nguyen et al 2019). This latter has been detected in the ISM (Cernicharo et al. 2012) but not the former for which the millimetric spectrum has been recently reported (Bermudez et al 2017). A proposed explanation was the high reactivity of •CH_2OH leading to a dimer, $HOCH_2CH_2OH$. This is consistent with the concomitant formation of an abundant isomer of ethylene glycol, the methoxymethanol for which the millimetric spectrum has been recorded and analyzed (Motiyenko et al. 2018) allowing its detection in the ISM (McGuire et al. 2017). In this case and following a similar mechanism, •CH_2OH reacts with the CH_3O• radical to form CH_3OCH_2OH.

$$CO \xrightarrow{+H} CHO \xrightarrow{+H} H_2CO \xrightarrow{+H} CH_2OH$$

$$CO \xrightarrow{+H} CHO \xrightarrow{+H} H_2CO \xrightarrow{+H} CH_3O$$

$$CH_3O + CH_2OH \rightarrow CH_3OCH_2OH$$

For mechanism 2, we have clearly demonstrated (Leroux et al 2020) that the hydrogenation of glyoxal does not lead to glycolaldehyde but to CO and H_2CO. In this context, looking for links between glyoxal and glycolaldehyde, similar experiments have been carried out in solid phase by Butscher et al. (2017) by investigating the formation and reactivity of HCO through VUV photolysis of H_2CO. They observed the efficient formation of HCO at 13 K and its consumption in the 50-70 K temperature range to form mainly glycolaldehyde and ethylene glycol, but not glyoxal. They conclude that while CHO + CH_2OH and CH_2OH + CH_2OH thermally induced radical reactions lead to $CHOCH_2OH$ and $HOCH_2CH_2OH$, respectively, CHO + CHO recombination would lead to H_2CO and CO rather to CHOCHO. However, mechanism 2 consists of three reaction pathways: the formation of glyoxal through CHO + CHO radical recombination, the hydrogenation of glyoxal to form glycolaldehyde and then the hydrogenation of glycolaldehyde to form ethylene glycol. The first and the second reactions would be rejected by the two experimental studies carried out by Butscher et al. (2017), and Leroux et al. (2020), respectively. We show in this paper that the third reaction emphasizing a link between glycolaldehyde and ethylene glycol through hydrogenation processes occurs under our experimental conditions. Consequently, in the interstellar medium, starting from CHO and CH_2OH as precursors, CHO + CH_2OH and CH_2OH + CH_2OH radical recombination would form $CHOCH_2OH$ and $HOCH_2CH_2OH$ respectively; then the hydrogenation reactions would be a source leading to an increase of the amounts of ethylene glycol and to a decrease of those of glycolaldehyde. These results are in good agreement with different astronomical observations which show simultaneous detections of glycolaldehyde and ethylene glycol in the galactic center Sgr B2 (Hollis et al. 2000; Hollis et al. 2002) and in solar-type protostar NGC 1333 IRAS2A (Maury et al. 2014; Coutens et al. 2015) with abundance ratios $HOCH_2CH_2OH/CHOCH_2OH$ ranged between 1 and 15 (Rivilla et al. 2017). This ratio varies in gas phase between 3 and 6 in NGC 1333 IRAS2A class 0 protostar and it is approximately 1 in IRAS 16293−2422 class 0 protostar (Jørgensen et al. 2012). The observation of different abundance ratios in favor of $HOCH_2CH_2OH$ and the presence of glycolaldehyde and ethylene glycol in the same astrophysical environments which are dominated by hydrogenation processes could indicate a chemical link between the two species through H-addition reactions.

6. Conclusion

In the present study, we have performed under ISM conditions the hydrogenation of glycolaldehyde, monitored by IR spectroscopy and mass spectrometry, in order to validate or

invalidate the astrophysical models showing a chemical link between saturated and unsaturated organic molecules. In order to emphasize the formation of $HOCH_2CH_2OH$ through $CHOCH_2OH$ + H solid state reaction, the difference spectrum after and before H-bombardments of $CHOCH_2OH$ ice has been compared to a reference spectrum corresponding to ethylene glycol ice formed at 10 K. Such a comparison allowed to support the consumption of $CHOCH_2OH$ and the formation of ethylene glycol through the IR detection of OH, CH, CO and CC stretching modes. Additionally, the thermal programmed desorption coupled with mass spectrometry confirms clearly the formation of $HOCH_2CH_2OH$ during the hydrogenation of $CHOCH_2OH$. Our results thus corroborate the theoretical predictions which suggest that glycolaldehyde could be a precursor of ethylene glycol in interstellar regions where the H-addition reactions predominate.

Data availability

The data of this paper will be shared on reasonable request to the corresponding author.

References

Alvarez-Barcia S., Russ P., Ka¨stner J., Lamberts T., 2018, MNRAS, 479, 2007
Beltran M. T., Codella C., Viti S., Neri R., Cesaroni R., 2009, ApJ, 690, L93 Bennett C. J., Kaiser R. I., 2007, ApJ, 661, 899
Bermudez C., Bailleux S., Cernicharo J., 2017, A&A 598, A9
Biver N. et al., 2014, A&A, 566, L5
Biver N. et al. 2015, Sci. Adv., 1, e1500863
Bleda E. A., Yavuz I., Altun Z., Trindle C., 2012, Int. J. Quantum Chem., 113, 1147
Boamah M. D. et al. 2014, Faraday Discuss., 168, 249
Boyer M. C., Rivas N., Tran A. A., Verish C. A., Arumainayagam C. R., 2016, Surf. Sci., 652, 26
Breslow R., 1959, Tetrahedron Lett., 1, 22
Brouillet N., Despois D., Lu X.-H., Baudry A., Cernicharo J., Bockele´e-Morvan D., Crovisier J., Biver N., 2015, A&A, 576, A129 Butscher T., Duvernay F., Theule P., Danger G., Carissan Y., Hagebaum-Reignier D., Chiavassa T., 2015, MNRAS, 453, 158 Butscher T., Duvernay F., Rimola A., Segado-Centellas M., Chiavassa T., 2017, Phys. Chem. Chem. Phys., 19, 2857
Butlerow A., 1861, Justus Liebigs Ann. Chem., 120, 295
Carbonniere P., Pouchan C., 2012, Theor. Chem Acc., 131, 1183
Cernicharo J., Marcelino N., Roueff E., Gerin M., Jime´nez-Escobar A., Mun˜oz-Caro G. M., 2012, ApJ, 759, L43
Coutens A., Persson M. V., Jørgensen J. K., Wampfler S. F., Lykke J. M., 2015, A&A, 576, A5
Crovisier J., Bockele´e-Morvan D., Colm P., Biver N., Despois Lis D. C., 2004, A&A, 418, L35

Fedoseev G., Cuppen H. M., Ioppolo S., Lamberts T., Linnartz H., 2015, MNRAS, 448, 1288
Fuchs G.W. et al., 2006, Faraday Discuss, 133, 331
Fuente A. et al. 2014, A&A, 568, A65
Gerakines P. A., Schutte W. A., Ehrenfreund P., 1996, A&A, 312, 289
Goesmann F. et al. 2015, Science, 349, aab0689
Halfen D. T., Apponi A. J., Woolf N., Polt R., Ziurys L. M., 2006, ApJ, 639, 237
Hollis J. M., Lovas F. J., Jewell P. R., 2000, ApJ, 540, L107
Hollis J. M., Lovas F. J., Jewell P. R., Coudert L. H., 2002, ApJ, 571, L59
Hollis J. M., Jewell P. R., Lovas F. J., Remijan A., 2004, ApJ, 613, L45
Hollis J. M., Vogel S. N., Snyder L. E., Jewell P. R., Lovas F. J., 2001, ApJ, 554, L81
Hudson R. L., Moore M. H., Cook A. M., 2005, Adv. Space Res., 36, 184
Islam S., Bucˇar D.-K., Powner M. W., 2017, Nat. Chem., 9, 584
Jørgensen J. K., Favre C., Bisschop S. E., Bourke T. L., Schmalzl M., van Dishoeck E. F., 2012, ApJ, 757, L4 Krim L., Jonusas M., 2019, Low Temp. Phys., 45, 710
Leroux K., Krim L., 2020, MNRAS, 500, 1188
Leroux K., Guillemin J.-C., Krim L., 2020, MNRAS, 491, 289
Le Roy L. et al. 2015, A&A, 583, A1
Maury A. J. et al. 2014, A&A, 563, L2
McGuire B. A. et al. 2017, ApJ, 581, L46
Motiyenko R., Margules L., Despois D., Guillemin J.-C., 2018, Phys. Chem. Chem. Phys., 20, 5509 Nguyen T. L., Ruscic B., Stanton J. F. 2019, J. Chem. Phys., 150, 084105
Pirim C., Krim L., 2011, Phys. Chem. Chem. Phys., 13, 19454
Potapov A., Jager C., Henning T., 2018, ApJ, 865, 58
Requena-Torres M. A., Martın-Pintado J., Martın S., Morris M.R., 2008, ApJ., 672, 352
Rivilla V. M., Beltra´n M. T., Cesaroni R., Fontani F., Codella C., Zhang Q., 2017, A&A, 598, A59 Sawodny W., Niedenzu K., Dawson J. W., 1967, Spectrochim. Acta A, 23, 799
Taquet V., Lopez-Sepulcre A., Ceccarelli C., Neri R., Kahane C., Charnley S. B., 2015, A&A, 804, 81 Wolff A.J., Carlstedt C., Brown W.A., 2007, J. Phys. Chem. C, 111, 5990
Woods P. M., Slater B., Raza Z., Viti S., Brown W. A., Burke D. J., 2013, ApJ, 777, 90